PROCEEDINGS OF SCIENCE

$B \to K^* \ell\ell$ and rare decays at CMS

Alessio Boletti[*] [†]
Universita' degli Studi di Padova & INFN
E-mail: alessio.boletti@cern.ch

The results of analyses involving rare decays of B mesons, performed using the data collect by the CMS experiment in pp collisions at $\sqrt{s} = 7$ TeV and 8 TeV, are presented.
Firstly, the angular analysis of the decay $B^0 \to K^* \mu^+ \mu^-$ with the 2012 data is introduced. The forward-backward asymmetry of the muons, the K^* longitudinal polarization fraction, and the differential branching fraction are determined as a function of the dimuon invariant mass squared. The results are in good agreement with the standard model expectations.
Then, the analysis of the $B_s^0 \to \mu^+ \mu^-$ and $B^0 \to \mu^+ \mu^-$ rare decays is presented. An excess is found for the B_s^0 decay and the measurement $\mathscr{B}(B_s^0 \to \mu^+ \mu^-) = (3.0^{+1.0}_{-0.9}) \times 10^{-9}$ is performed. No significant excess is found for the B^0 decay and the upper limit $\mathscr{B}(B^0 \to \mu^+ \mu^-) < 1.1 \times 10^{-9}$ at 95 % confidence level is set.

16th International Conference on B-Physics at Frontier Machines
2-6 May 2016
Marseille, France

[*] Speaker.
[†] on behalf of the CMS Collaboration

PoS(BEAUTY2016)045

1. Introduction

Rare decays are those processes that are highly suppressed according to the Standard Model (SM) predictions. These decays are an excellent laboratory to probe the SM, since possible contributions from new physics would have an amplitude comparable with the expected one and it would considerably modify the features of the process. The Compact Muon Solenoid (CMS) Collaboration gave a significant contribution to the study of two heavy flavour physics rare decays: the $B^0_{d(s)} \to \mu\mu$ decays [1] and the $B^0 \to K^*(892)^0\mu\mu$ decay [2, 3].

2. $B^0 \to K^*(892)^0\mu^+\mu^-$ angular analysis

The flavour changing neutral current decay $B^0 \to K^*(892)^0\mu^+\mu^-$ is particularly fertile for new phenomena searches thanks to the modest theoretical uncertainties, due to the semileptonic final state. Furthermore, this decay is forbidden at tree level and the leading order diagrams that mediate this process are the box and penguin ones. This fact makes this decay channel very sensitive to virtual contributions of new particles.

In this three body decay, there are two angular parameters that have small theoretical uncertainties: the forward-backward asymmetry of the muons, A_{FB}, and the K^{*0} longitudinal polarization fraction, F_L. These parameters, along with the differential branching fraction $\mathrm{d}B/\mathrm{d}q^2$, can be determined as a function of the dimuon invariant mass squared, q^2, and compared with SM expectations.

The CMS collaboration performed two analyses [2, 3] to study this decay, using data collected from proton-proton collisions at the Large Hadron Collider (LHC) with the CMS experiment in 2011 and 2012 at a center-of-mass energy of 7 TeV and 8 TeV, respectively. A combination of these two results is also performed. Only the analysis performed on the 2012 dataset, corresponding to an integrated luminosity of $20.5 \pm 0.5\,\mathrm{fb}^{-1}$, is presented here.

2.1 Angular parametrization

The considered final state contains two opposite charged muons and a kaon and a pion as the decay products of the K^{*0}. The three angular variables that completely describe the decay are: the angle between the kaon momentum and the direction opposite to the B^0 in the K^{*0} rest frame, θ_K, the angle between the positive (negative) muon momentum and the direction opposite to the B^0 ($\bar{B}^0$) in the dimuon rest frame, θ_l, and the angle between the plane containing the two muons and the plane containing the kaon and the pion, ϕ.

Contribution from spinless $K\pi$ combination is present, although the $K\pi$ invariant mass is imposed to be consistent with the K^{*0} one. The fraction of S-wave contribution is parametrized as F_S and the interference contribution between S-wave and P-wave is A_S.

Since the A_{FB} and F_L parameters do not depend on ϕ and the efficiency is reasonably constant in this variable, it is integrated out in order to reduce the number of free angular observables.

2.2 Control samples and background events

The range of q^2 considered goes from $1\,\mathrm{GeV}^2$ to $19\,\mathrm{GeV}^2$ and it is divided in nine bins of different width. The fifth and the seventh bins correspond to the mass resonances of J/ψ and

ψ'. The former ranges from $8.68\,\mathrm{GeV}^2 < q^2 < 10.09\,\mathrm{GeV}^2$ and it is used as normalization channel to compute the branching fraction measurement. The latter resonance bin covers the range $12.86\,\mathrm{GeV}^2 < q^2 < 14.18\,\mathrm{GeV}^2$ and it is used as control channel.

After the selection cuts and the K^{*0} mass requirement, a further cut is applied to reduce the feed-through from the resonant channel caused by photons radiated from the muons. The background in the final sample is then mostly due to combinatorics. The small contribution from the remaining resonant-channel background is taken into account as a systematic uncertainty.

2.3 Fit algorithm

In order to extract the values of the angular parameters and the signal and background yield, a simultaneous unbinned maximum likelihood fit to the B^0 recontructed mass, to the $\cos\theta_K$ and to the $\cos\theta_l$ distributions is performed for each q^2 bin.

The $p.d.f.$ used to fit the data is

$$\mathrm{PDF}(m,\theta_K,\theta_l) = \Upsilon_S^C\left[S^C(m)S^a(\theta_K,\theta_l)\varepsilon^C(\theta_K,\theta_l) + \frac{f^M}{1-f^M}S^M(m)S^a(-\theta_K,-\theta_l)\varepsilon^M(\theta_K,\theta_l)\right] + \Upsilon_B B(m)B^{\theta_K}(\theta_K)B^{\theta_l}(\theta_l)$$

where the first contribution corresponds to the correctly-tagged signal events, the second one to the wrongly-tagged signal events, where the pion track and the kaon track are misidentified, and the third contribution correspond to background events.

The parameters Υ_S^C and Υ_B are the yields of correctly tagged signal events and background events, respectively. The parameter f^M is the fraction of mistagged signal events. The signal mass shapes, $S^C(m)$ and $S^M(m)$, are each the sum of two Gaussian functions and describe the mass distribution for correctly tagged and mistagged signal events, respectively. The function $S^a(\theta_K,\theta_l)$ describes the signal in the two-dimensional space of the angular observables. The combination $\Upsilon_B B(m)B^{\theta_K}(\theta_K)B^{\theta_l}(\theta_l)$ is obtained from B^0 sideband data and describes the background in the space of (m,θ_K,θ_l), where the mass distribution is an exponential function and the angular distributions are polynomials ranging from second to fourth degree, depending on the q^2 bin and the angular variable. The functions $\varepsilon^C(\theta_K,\theta_l)$ and $\varepsilon^M(\theta_K,\theta_l)$ are the efficiencies in the 2D space of the angular observables for correctly tagged and mistagged signal events, respectively.

2.4 Results

The fit results are plotted in figure 1 and compared with the SM expectations [4, 5]. Controlled theoretical predictions are not available near the resonance regions.

3. Measurement of the $B_s^0 \to \mu\mu$ branching fraction and search for the $B^0 \to \mu\mu$ decay

The $B_s^0 \to \mu^+\mu^-$ and $B^0 \to \mu^+\mu^-$ are FCNC decays, suppressed by many factors according to the SM predictions. In the SM, the very small predicted branching fraction are $\mathscr{B}(\mathrm{B_s^0} \to \mu^+\mu^-) = (3.66 \pm 0.23) \times 10^{-9}$ and $\mathscr{B}(\mathrm{B^0} \to \mu^+\mu^-) = (1.06 \pm 0.09) \times 10^{-10}$ [7, 8].

The CMS collaboration performed the analysis of these decays using the data sample collected in pp collsion at $\sqrt{s} = 7\,\mathrm{GeV}$ and $\sqrt{s} = 8\,\mathrm{GeV}$, for integrated luminosities of 5 fb^{-1} and 20 fb^{-1}, respectively.

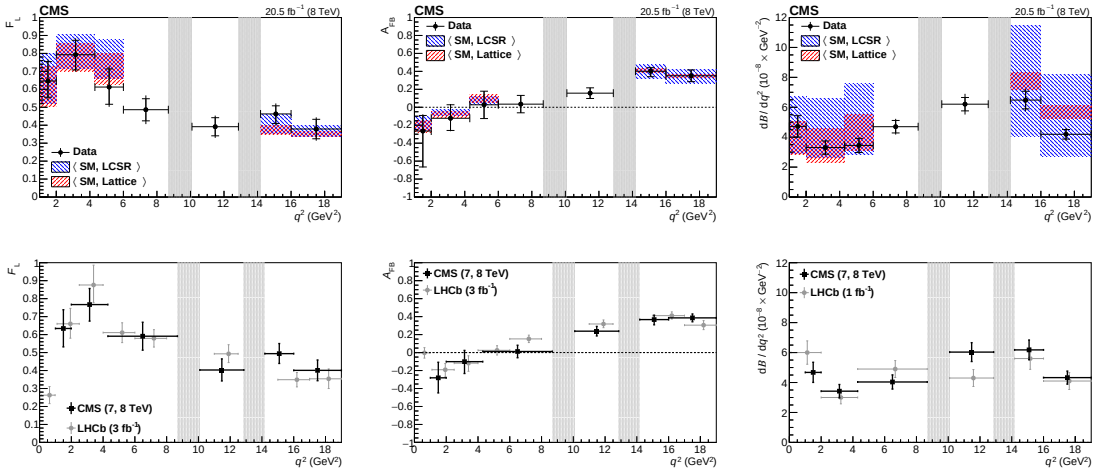

Figure 1: On top plots, the results of the measurement of F_L (left), A_{FB} (centre) and $\mathrm{d}B/\mathrm{d}q^2$ (right) versus q^2. The statistical uncertainty is shown by inner error bars, while the outer error bars give the total uncertainty. The vertical shaded regions correspond to the J/ψ and ψ' resonances. The other shaded regions show the SM prediction as a continuous distribution and after rate-averaging across the q^2 bins (<SM>) to allow direct comparison to the data points. In bottom plots the combination of the results with 2011 and 2012 datasets and the comparison with the most recent LHCb measurement [6].

3.1 Analysis strategy

Until the selection criteria are complitely established, the data in the signal region $5.20 < m_{\mu\mu} < 5.45\,\mathrm{GeV}$ are kept blind, in order to avoid possible biases.

The main background in this analysis is due to combinatorial semileptonic decays of two B hadrons in the event. The contribution of these events are estimated in data by the analysis of dimuon mass sidebands, and extrapolated into the signal region. Another source of background contamination are the $B \to h\mu\nu$, $B \to h\mu\mu$, and $\Lambda_b \to h\mu\nu$ semileptonic decays, where the hadron is mis-identified as a muon. Finally, also the rare peacking hadronic decays $B \to hh$, where both the hadrons are mis-identified, are a source of background. The contribution of the last two sources are estimated from Monte Carlo (MC) simulations.

Two samples of B meson decays are used in the analysis. In order to reduce the uncertainties from the $b\bar{b}$ production cross section and the luminosity, the $B^+ \to J/\psi K^+$ decay is used as normalization channel and its well known branching fraction [9] is used. Furthermore, a sample of $B_s^0 \to J/\psi\phi$ is used as control channel to evaluate differences in fragmentation between B^+ and B_s^0 and to validate the B_s^0 production in the MC simulations.

The events selection at trigger level requires two muons candidates in the muon detector, with compatible hits in the silicon tracker and an invariant mass compatible with the B_s^0 mass. Events are selected offline requiring two well-reconstructed muons consistent with the pair that triggered the event. A further selection with thigher requirements is applied, in order to reduce the background contamination. Cuts are applied on the direction of the dimuon system with respect to the primary vertex of the events, on the flight length significance, and on the distance of closest approach of the two muons. Furthermore, a multivariate identification criterion is applied to enhance the identification of muon against mis-identified charged hadrons like pions, kaons and protons. Several

input informations are used, combining kinematic variables, tracker-based informations, muon detector track informations, and combined features of the fit of both tracker and muon spectrometer hits. A boosted decision tree (BDT) is trained using a simulated $B_s^0 \to \mu\mu$ signal sample and simulated background samples of B mesons decays to pions and kaons. The resulting mis-identification probability is $(0.5-1.3)\times 10^{-3}$, $(0.8-2.2)\times 10^{-3}$, and $(0.4-1.5)\times 10^{-3}$ for pions, kaons, and protons respectively, where the ranges are due to different pseudorapidity, running period, and particle momentum values.

A kinematic fit is performed on the two muon tracks, costraining them to a common vertex and then a selection cut is applied, requiring the dimuon invariant mass in the range $4.9 < m_{\mu\mu} < 5.9\,\text{GeV}$. The mass resolution estimated from MC is about 32 MeV for events where the dimuon is produced in central region, and it is 75 MeV if the candidate B_s^0 is reconstructed at $|\eta| > 1.8$. Events are divided in two categories, according to the muon pseudorapidity. The barrel category contains the events where both muons are in the central region ($|\eta| < 1.4$), while the endcap category contains the events where at least one muon is in the forward region ($|\eta| > 1.4$). A final multivariate selection is then applied, to separate the signal from the non-peaking background. Different BDT are trained for different data-taking periods and for barrel and endcap categories, using a simulated $B_s^0 \to \mu\mu$ signal sample and the $m_{\mu\mu}$ sidebands of the data as background. A set of 12 input variables is used, combining informations related to topological and kinematic quantities of the event. The good agreement between data and simulation is verified for all the input variables and the output of each BDT method is proved to be insensitive to the dimuon invariant mass and to the pileup.

Two analysis methods are applied, in order to achive the best sensitivity for different measured quantities. The first one is optimised to extract the best upper limit on the $\mathscr{B}(B^0 \to \mu^+\mu^-)$, in the case that non significant excess is found over the background expectation, and the second method provides the best sensitivity in the measurement of the branching fractions. In the first one, referred as 1D-BDT, a single cut on the BDT output is defined in each of the four signal categories and for two mass regions around B^0 and B_s^0 masses. These cuts are chosen to optimize the signal sensitivity $S/\sqrt{S+B}$, where S and B are the expected number of signal and background events, respectively. In the second method, for each signal category a set of cuts on the BDT output is defined, such that in each BDT region the same signal yield is expected. Then, a simultaneous unbinned maximum-likelihood fit to the dimuon invariant mass, $m_{\mu\mu}$, is performed over these regions to extract the signal and background yields. The branching fraction is measured relatively to the normalization channel, using the value $\mathscr{B}(B^+ \to J/\psi K^+) = (6.0 \pm 0.2)\times 10^{-5}$. The ratio of the b-quark to hadronize into B^+ to B_s^0 measured by the LHCb Collaboration [10], $f_u/f_s = 0.256 \pm 0.020$, is used.

3.2 Results

An excess compatible with $B_s^0 \to \mu^+\mu^-$ signal is observed, as shown in Figure 2. The estimated branching fraction for this decay is $\mathscr{B}(B_s^0 \to \mu^+\mu^-) = (3.0^{+1.0}_{-0.9})\times 10^{-9}$, where statistical and systematic uncertainties are combined. No significand excess is found for the $B^0 \to \mu^+\mu^-$ contribution, so it is treated as nuisance parameter in the fit procedure. The 1D-BDT method is used to extract the upper limit $\mathscr{B}(B^0 \to \mu^+\mu^-) < 1.1\times 10^{-9}$ at 95% confidence level, using the CL_s approach.

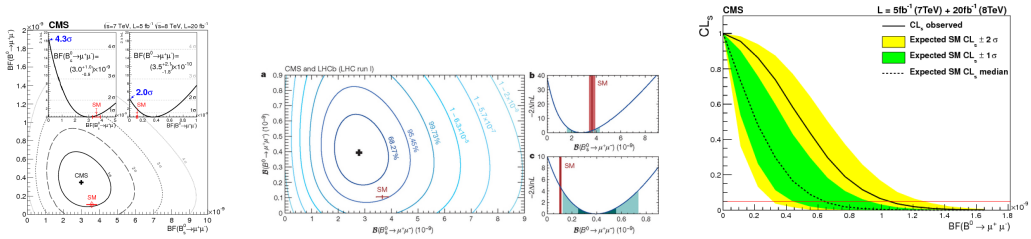

Figure 2: Scan of the likelihood ratio of the $\mathscr{B}(B_s^0 \to \mu\mu)\mathscr{B}(B^0 \to \mu\mu)$ plane for the CMS analysis (left) and for the CMS+LHCb combination (centre). In the small box in the figure, the likelihood ratio scan for the two branching fractions when the other is considered a nuisance parameter to the fit. The observed and expected CL_s for the $\mathscr{B}(B^0 \to \mu\mu)$ decay (right) as a function of the assumed branching fraction.

This measurement has also been combined [11] with the LHCb analysis. In this combination a simultaneous unbinned maximum-likelihood fit is performed on the two datasets. The decay $B_s^0 \to \mu^+\mu^-$ is observed and its branching fraction is found to be $\mathscr{B}(B_s^0 \to \mu^+\mu^-) = (2.8^{+0.7}_{0.6}) \times 10^{-9}$. Furthermore an excess compatible with the $B^0 \to \mu^+\mu^-$ signal is measured, providing a branching fraction of $\mathscr{B}(B^0 \to \mu^+\mu^-) = (3.9^{+1.6}_{1.4}) \times 10^{-10}$.

4. Conclusions

The angular analysis of the $B^0 \to K^{*0}\mu^+\mu^-$ decay is presented. The measured values of A_{FB}, F_L and of the differential branching fraction $\mathrm{d}B/\mathrm{d}q^2$ are compatible with SM predictions.

The analysis of the $B_s^0 \to \mu^+\mu^-$ decay is also presented. An excess is found in this channel, leading to the measurement of its branching fraction. The results of the CMS and LHCb combined analysis are reported, with the first observation of the $B_s^0 \to \mu^+\mu^-$ decay and the measurement of an excess compatible with the $B^0 \to \mu^+\mu^-$ decay. All the measured branching fractions are in agreement with SM expectations.

References

[1] CMS Collaboration, *Phys. Rev. Lett.* **111** (2013) 101804

[2] CMS Collaboration, *Phys. Lett. B* **727** (2013) 77

[3] CMS Collaboration, *Phys. Lett. B* **753** (2016) 424-448

[4] C. Bobeth, G. Hiller, and D. van Dyk, *JHEP* **07** (2010) 098

[5] C. Bobeth, G. Hiller, and D. van Dyk, *Phys. Rev. D* **87** (2012) 034016

[6] LHCb Collaboration, *JHEP* **02** (2016) 104

[7] A. J. Buras, J. Girrbach, D. Guadagnoli, and G. Isidori, *Eur. Phys. J.*, **C72** (2012) 2172

[8] K. De Bruyn et al., *Phys. Rev. Lett.*, **109** (2012) 041801

[9] K. A. Olive et al., *Chin. Phys.*, **C38** (2014) 090001

[10] LHCb Collaboration, *JHEP*, **04** (2013) 001

[11] CMS and LHCb Collaborations, *Nature*, **522** (2015) 68